

All Things Homunculus

Nathan Smith

Abstract The “Homunculus” nebula around Eta Carinae is one of our most valuable tools for understanding the extreme nature of episodic pre-supernova mass loss in the most massive stars, perhaps even more valuable than the historical light curve of η Car. As a young nebula that is still in free expansion, it bears the imprint of its ejection physics, making it a prototype for understanding the bipolar mass loss that is so common in astrophysics. The high mass and kinetic energy of the nebula provide a sobering example of the extreme nature of stellar eruptions in massive stars near the Eddington limit. The historical ejection event was observed, and current parameters are easily measured due to its impressive flux at all wavelengths, so the Homunculus is also a unique laboratory for studying rapid dust formation and molecular chemistry, unusual ISM abundances, and spectroscopy of dense gas. Since it is relatively nearby and bright and is expanding rapidly, its 3-D geometry, kinematics, and detailed structure can be measured accurately, providing unusually good quantitative constraints on the physics that created these structures. In this chapter I review the considerable recent history of observational and theoretical study of the Homunculus nebula, and I provide an up-to-date summary of our current understanding, as well as areas that need work.

1 EARLY OBSERVATIONS AND PROPER MOTIONS

Eta Carinae was first recognized as a spatially extended object in 1900–1930 by Innes, van den Bos, and Voûte, who noted visual companion objects less than $2''$ from the star (see [135, 41, 95, 111]). Around 1950 the structure was recognized as nebular by Thackeray and by Gaviola [135, 41]. Gaviola named it “the Homunculus” because on photographic plates it resembled a small plump man (Fig. 1). The

Nathan Smith
Astronomy Department, University of California, 601 Campbell Hall, Berkeley, CA 94720 e-mail: nathans@astro.berkeley.edu

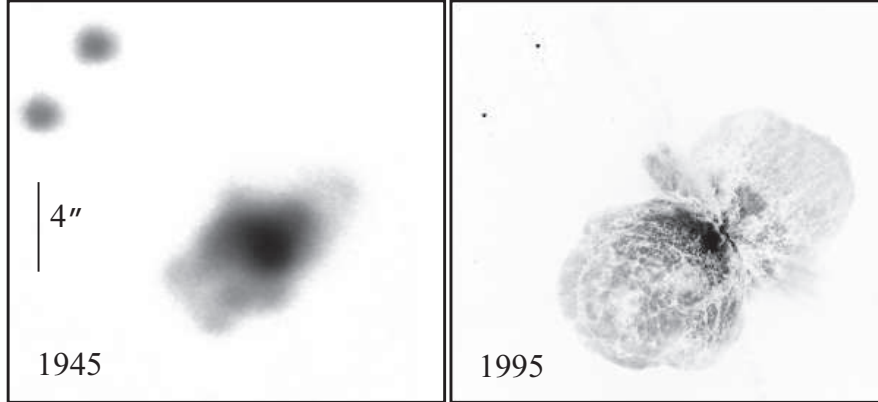


Fig. 1 Two visual images of the Homunculus, printed with the same spatial scale. *Left*: Gaviola’s blue photograph, from an original photographic plate that was digitally scanned by the author [41, 111]. *Right*: A red-wavelength image obtained 50 yr later with the *HST* [80].

earliest visible features were mostly in the equatorial parts of the bipolar configuration. The polar lobes had a diameter of $5\text{--}10''$ in 1900–1940, but the relatively low surface brightness of their outer extremities made them inconspicuous in the glare of the $3''$ central region (see [41, 20]). During the 1940’s the lobes may have brightened more than the central core region did [136, 27]. This brightening is probably an important clue to η Car’s recovery from the 1843 eruption, but it is difficult to infer physical information from the scant historical record.

Early measurements of the Homunculus’ expansion showed that it was ejected in the mid-to-late 19th century [41, 95, 42]. The obvious implication, that it was created in the Great Eruption, was later verified by measurements using data from *HST* and with higher spatial resolution or longer temporal baselines [16, 111, 81]. Thus we know reliably that the bulk of the Homunculus nebula was ejected in a relatively short time interval during the 1840s. It therefore contains some of our most valuable information about the Eruption. This doesn’t necessarily mean, however, that *all* the ejecta came from that event. A number of features appear to have been ejected later, perhaps in the 1890 secondary eruption. These are discussed later.

2 THE BRIGHTEST OBJECT IN THE MID-INFRARED SKY

One of the most important developments in understanding η Car was the recognition that it is extremely luminous at infrared (IR) wavelengths. In 1968–1969 Neugebauer & Westphal discovered a strong near-IR excess at $1\text{--}3\ \mu\text{m}$, and then, more important, extremely luminous mid-IR radiation at $5\text{--}20\ \mu\text{m}$ [82, 148]. This led to our present understanding of the energy budget as that of a very luminous star en-

shrouded by circumstellar dust, which reprocesses the UV/visual luminosity into thermal IR radiation [90, 91, 18, 98, 65].

In subsequent decades, the Homunculus was a favorite target for mid-IR astronomers because it was bright and spatially extended. Early measurements of the spectral energy distribution (SED) established a range of dust temperatures, 400 to 200 K, a large gas mass of at least a few M_{\odot} , strong and broad silicate emission at $9.7 \mu\text{m}$, unusually large grains with radii of roughly $1 \mu\text{m}$, and a lack of strong fine-structure emission lines [43, 96, 133, 64, 1, 6, 5, 75]. The reasoning for large grains was based mainly on dust temperatures near the blackbody values for the projected radii of extended features in mid-IR maps, and on the broad silicate feature [76, 97], but this also agreed with the unusually low reddening/extinction ratio at shorter wavelengths (e.g., [98]). The dusty Homunculus acts as a calorimeter, providing us with an estimate of the star’s total luminosity $L \approx 5 \times 10^6 L_{\odot}$. This is more robust than for most other massive stars, because it does not require a model-dependent spectral extrapolation to UV wavelengths.

The Homunculus showed complex spatial structure in even the earliest IR drift scans and raster maps that used single-element detectors with $1\text{--}2''$ spatial resolution. Several authors noted an elongated, double-peaked, or torus-like structure in the warm inner core, plus a more extended cooler halo [59, 77, 11, 7, 100, 3].

In the mid-1980s Hackwell, Gehrz, and Grasdalen made a mid-IR raster map of the Homunculus, which first clearly delineated the limb-brightened structure of the two hollow polar lobes (described as “osculating spheres”), the outer boundary of the mid-IR emitting structure, and the complex multi-temperature and multi-peaked structure of the core region [51].

The advantage of mid-IR imaging of the lobes, compared to reflected light in visual-wavelength images, is that the thermal dust radiation in the mid-IR is optically thin, so we can see that the lobes are hollow and that condensations exist in the obscured core region. Subsequent imaging with array detectors on 4m-class telescopes improved upon the spatial resolution (especially in the core), the sensitivity, and the wavelength coverage, but confirmed the basic structure [103, 111, 120, 93, 78, 92, 55]¹. So far, the only high-quality mid-IR polarimetric imaging was presented by Aitken et al. ([2]; see also [10]), which revealed suggestive evidence of grain alignment from a possible swept-up ambient magnetic field, or a strong original field in the star’s atmosphere before the eruption. Our mid-IR view of the Homunculus improved greatly with the advent of 8m-class telescopes [122, 123, 12], because at long wavelengths like $10\text{--}20 \mu\text{m}$, the increased diffraction limit of larger telescopes is critical. These modern IR observations will be discussed along with our modern view of the structure of the nebula below.

¹ Note, however, that some of the morphological interpretations in these studies were contradicted by later observations.

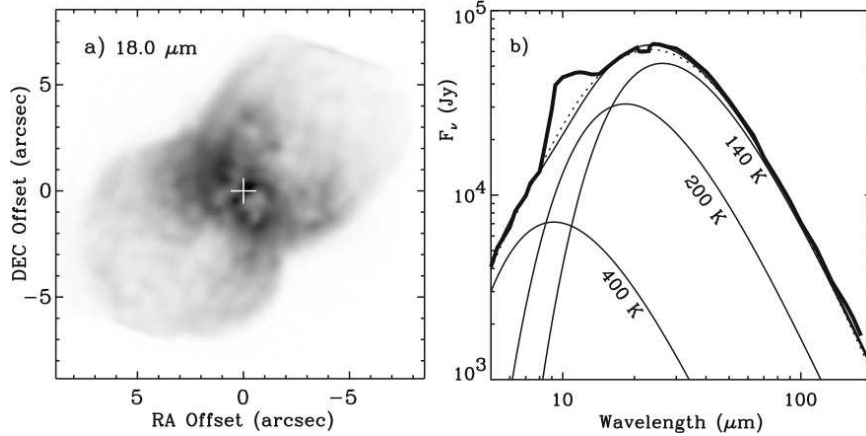


Fig. 2 (a) An 18 μm image of the Homunculus taken with the 6.5-m Magellan telescope [123]. (b) the mid-IR SED of η Car with the 140 K, 200 K, and warmer component fits used to derive the mass in the polar lobes [123].

3 MASS AND KINETIC ENERGY OF THE HOMUNCULUS

As noted earlier, the Homunculus is potentially our most valuable probe of the 19th century eruption and this class of stellar outbursts, because with the knowledge from proper motion studies that it was indeed ejected in that event, the Homunculus provides us with two essential quantities: the ejected mass and its kinetic energy.

The usual way of measuring this mass is to estimate the *dust* mass that is needed to produce the IR emission, and then to multiply by a reasonable gas/dust mass ratio. With conventional silicate grain emissivities and gas/dust = 100, the observed 2–12 μm SED yields a Homunculus mass of 2–3 M_{\odot} , representing the ~ 200 K material in the polar lobes [14, 120]. This is consistent with the circumstellar extinction [19]. However, dense clumps which are opaque at visual wavelengths [33, 80] may contain additional mass that is under-represented in either type of estimate. For this reason, it can be problematic to deduce *both* the stellar luminosity and the ejecta mass from the same observed IR luminosity.²

Indeed, the mass estimate of 2–3 M_{\odot} that was adopted for many years is now known to be too small. More recent estimates from dust emission place the ejecta mass (assuming the same gas/dust mass ratio of 100) at *much higher* values of 12.5, 15, or even 20 M_{\odot} [123, 78]. This upward revision followed chiefly from high-quality measurements at far-IR wavelengths, which revealed a large mass of dust much cooler than 200 K [78, 123] (Fig. 2).

An important distinction must be noted regarding the location of this cool material. Morris et al. [78] fit the far-IR spectrum with dust at 110 K, and proposed

² Thus ref. [19] warned in 1997 that at least one of those parameters had presumably been underestimated by a then-unknown factor.

that it resides in a *pre-existing* massive disk or torus that pinched the waist of the Homunculus when it was formed in the Great Eruption. But Davidson & Smith [21] noted that any thermal source at 110 K must cover a much larger projected area in order to produce the observed IR flux, and that the torus-like structure was already known to be much warmer than 110 K. After discovering a thin outer shell of 140 K dust in high-resolution mid-IR images at 18–25 μm , Smith et al. [123] performed an independent analysis of the same far-IR data and found that it could be fit equally well with 140 K dust. They suggested instead that the large mass of more than $10 M_{\odot}$ exists in the polar lobes of the Homunculus, and that there is very little mass near the equator. This view had two critical implications: (1) the 1840s eruption ejected a large mass in an intrinsically bipolar flow, i.e., it was not shaped by pre-existing equatorial material; and (2) the $>10 M_{\odot}$ of material is moving very fast, with a kinetic energy of $10^{49.6}–10^{50}$ erg [123].

If the mass and kinetic energy values noted above are incorrect, they are probably *underestimates* because the dominant sources of error tend toward higher mass. The assumed gas/dust mass ratio of 100 is probably too low given that the ejecta are known to be C and O poor [22]. Potential optical depth effects, such as shielded cold grains in dense clumps, can hide additional mass. Recent observations at sub-mm wavelengths that are sensitive to the coldest material indicate 0.3–0.7 M_{\odot} of dust [44], implying 30–70 M_{\odot} of gas if gas/dust = 100 (although some of this emission may come from a more extended region). Independent of IR dust measurements, Smith & Ferland [113] estimated a large *gas* mass of 15–35 M_{\odot} for nebular models that allow H_2 molecules to survive near such a luminous star (though values near the lower end of the range are favored). So far this is the only estimate of the ejecta mass that does not rely on an assumed gas/dust ratio.

If η Car ejected as much as 20–30 M_{\odot} in a single event that lasted just a few years, this begins to strain the star’s available mass reservoir if the upper mass limit to stars really is around 150 M_{\odot} , especially if other events like the Great Eruption have happened once or twice in the past few thousand years. Such extreme values of the mass and kinetic energy underscore the profound influence of such high mass-loss events in the evolution of massive stars [116, 57], not to mention their potential role as precursors to the most luminous supernova explosions [127, 150]. The fact that they still have no theoretical explanation makes this one of the most pressing mysteries in astrophysics, which has not yet received the attention it deserves.

4 THE BI-POLAR LOBES

Since the Homunculus is the major product of the 1843 eruption, its shape, structure, mass, and energy are vital clues for the outburst mechanism and the origin of the bipolar shape that is so pervasive in astrophysics. This object has consistently been a favorite target of imaging and spectroscopic studies with ever-increasing resolution. But it has not yielded its secrets easily, and there has been a great deal of controversy over its true structure. Recent observations have helped.

4.1 *Imaging Studies of the Homunculus as a Reflection Nebula*

Although early drawings and photographs showed the polar lobes of the Homunculus [135, 41, 42], the familiar structure we recognize today was not clearly apparent. Some authors specifically described it as “bipolar” based on velocities and polarization [146, 71]. The first images to show detailed features of the polar lobes and especially the thin equatorial skirt were ground-based images shown by Duschl et al. [30]. Later Hubble Space Telescope images obtained with a carefully-chosen set of filters and dithered WFPC2 exposures provided a spectacularly sharp view of the Homunculus [80], and became among the most familiar and oft-reproduced images made with HST.³ The bipolar lobes appear remarkably symmetric in these images, although Morse et al. [80] remarked that a slight axial asymmetry can be perceived by simply rotating one of the familiar HST images by 180°. Multiple epochs of images with WFPC2 and HST’s ACS instrument have enabled detailed investigations of the proper motions and light variations in the nebula [33, 16, 121, 125, 126, 81, 69].

Some of the most notable results from these imaging data are: (1) intricate, mottled structure on the surfaces of the polar lobes [80], resembling convective solar granulation or vegetable-inspired comparisons, (2) the ragged, streaked appearance of material in the equatorial skirt [30, 19, 80], some of which seem to connect to more distant nebular features, and (3) the blue glow or Purple Haze [80, 126, 151], a near-UV fluorescent nebulosity in the core of the Homunculus, perhaps associated with the Little Homunculus or equatorial ejecta [107]. HST also revealed remarkable features inside and outside the lobes, reviewed in other chapters.

Although the Homunculus has structures similar to those seen in planetary nebulae, it is not a hot photoionized emission-line nebula. Instead it contains cool low-ionization gas, molecules, and dust grains. Its visual spectrum is a complex mixture of reflected starlight and intrinsic emission from low-ionization species such as [Fe II]; the former dominates visual-wavelength radiation at most locations [71, 53, 25, 124, 151]. The scattered light is linearly polarized, with a level of 20–40% at visual wavelengths [137, 138, 140, 146, 101, 102] and 15–30% in the near-IR [145]. Even the strong $H\alpha$ emission is mainly $H\alpha$ from the stellar wind, reflected by grains [72, 34, 124]. The surface brightness distribution is consistent with scattered starlight with moderately large optical depths [20]. The Homunculus has even been detected as a Thomson-scattering nebula at hard X-ray wavelengths when the central source fades [13].

Light scattered by the Homunculus affords us a unique opportunity to view the star from a range of directions. The UV/visual spectrum in the middle of the approaching SE polar lobe gives a nearly pure (albeit spectrally blurred) reflected spectrum of the star from a polar direction [23, 151]. Smith et al. [124] exploited this fact to derive a 3-D view of the latitude dependence in the stellar wind of η Car, once the 3-D shape and orientation of the nebula had been determined [25, 105].

³ [Ed. comment:] Ironically, the lobes are now easily recognizable as such when viewed through an ordinary telescope. Eta Car’s visual appearance has changed dramatically in the past 20 years.

Other than the Sun, this is perhaps the only opportunity in astrophysics where the spectrum of a star has been viewed from a range of known latitudes. Likely effects of rapid rotation and a companion star make this of significant interest.

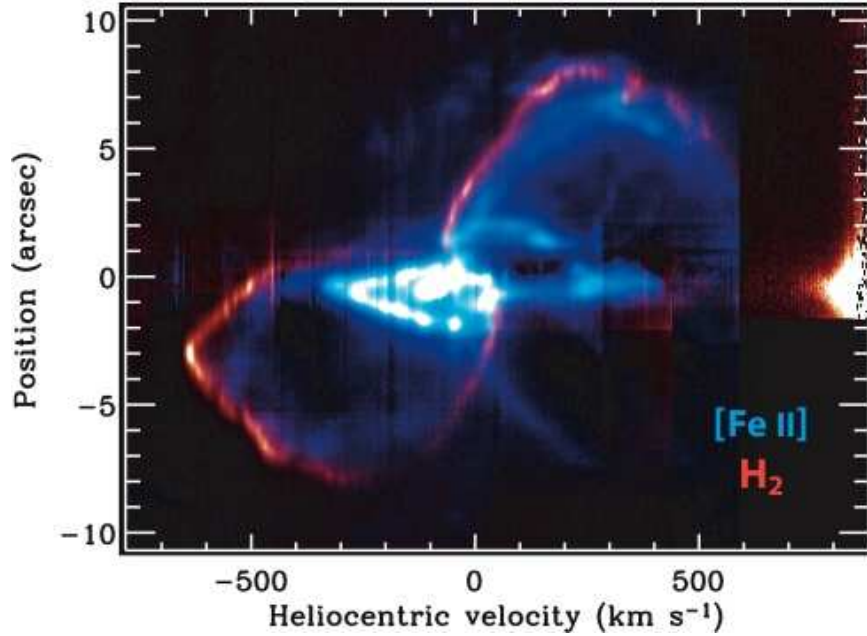


Fig. 3 Long-slit IR spectra of the Homunculus [108], showing the shape and detailed double-shell structure in H₂ (red; thin outer shell) and [Fe II] 1.644 μm (blue, thicker inner shell). [Fe II] emission from the Little Homunculus can also be seen [107].

4.2 Shape and Orientation of the Polar Lobes

Structures seen in images are only part of the picture. Kinematic information is needed to understand the true 3-D structure. Pioneering studies by Thackeray, Meaburn, and others combined proper motions with Doppler velocities to establish that the southeast lobe is tilted toward us and expanding away from the star with maximum speeds of roughly 650 km s^{-1} , and that the distance to η Car based on expansion is 2.0–2.5 kpc [138, 71, 53, 72, 4]. Hillier & Allen [53, 4] used long-slit spectra to probe the shape and expansion properties. They noted the distinction between narrow lines like [Ni II] and [Fe II] formed in the expanding nebula, as opposed to dust-scattered components of broad stellar-wind lines or narrow features arising near the star (see also [71, 72]). Together these studies reduced the kinematic ambiguities, and confirmed that the Homunculus is basically a Hubble flow with a

definite age. Today, with higher spatial resolution studies using HST/STIS spectra and high-resolution near-IR spectra, we have more accurate estimates of the inclination $i = 42^\circ$ (the tilt angle of the polar axis from our line of sight), the distance of 2.3 kpc [74, 25, 105, 108], and the lobe shapes.

For several years, the shape of the polar lobes was discussed in the context of three alternative models called the “double bubble” (two hollow osculating spheroids), “bipolar caps,” and a “double flask” [52]. Each found some justification in various aspects of the imperfect observational data. The hollow double-bubble model matched optical and mid-IR images that showed round, limb-brightened lobes [51, 72]. The double cap model emphasized that the polar regions appear optically thick while the side walls are more transparent [4]. The flask model had some advantages concerning polarization and kinematic properties [17]. In the end, better data made the distinctions between them largely irrelevant.

The Space Telescope Imaging Spectrograph (HST/STIS), with long-slit spectroscopy at high spatial resolution, provided the opportunity to improve upon the ground-based results. Davidson et al. [25] analyzed some of the same emission and reflection features as Hillier & Allen [53], obtaining a much better estimate of the shape and orientation of the nebula. A curious discrepancy appeared, however: polar lobe shapes derived from [Ni II] emission lines in STIS data were too narrow and short compared to those seen in images. This discrepancy was solved when the first long-slit near-IR spectra were taken into account [105], showing that images in scattered light corresponded to a thin outer shell seen in H_2 emission, while the [Ni II] emission represented a layer interior to that. This double-shell structure is discussed below.

Currently the best estimate of the 3-D shape, structure, and orientation of the polar lobes is provided by near-IR, long-slit echelle ($R=60,000$) spectra of H_2 emission [108]. The H_2 traces the dense outer dust shell (see Fig. 3) where most of the mass resides, and which is seen as the reflection nebula in images. The shape and expansion speed are now known with a precision of roughly 2–3% at all latitudes in the polar lobes. The limiting factor in this study is not the observational precision, but intrinsic variations and modulations in the lobes themselves, as well as the assumption that the nebula is axisymmetric.

In other words, the present model for the shape [108] is as definitive as the configuration will allow. Ground-based IR spectra were even better suited to the task than STIS for three reasons: (1) their spatial resolution is almost as good as STIS, but the velocity resolution of the long-slit echelle spectra is much higher; (2) they trace unique IR molecular hydrogen emission from the outer shell instead of atomic gas in the inner shell (Fig. 3), and (3) at near-IR wavelengths one can see all the way through to the far walls of the polar lobes, mitigating optical-depth effects. Thus we now know the 3-D shape of the nebula to high enough precision to constrain physical models for its formation.

4.3 Density and Ionization Structure of the Polar Lobes

In addition to the overall shape, recent observations from large ground-based telescopes and *HST* have significantly advanced our understanding of the detailed density and ionization structure of the Homunculus. Until recently, the walls of the polar lobes were generally assumed to have a thickness of $\sim 10\%$ of their radius [51, 120], and aside from the clumpy structure in *HST* images, not much more was known about their detailed structure.

Now we know that the walls actually have a well-defined double-shell structure (Fig. 3; [108]), where most of the mass is in a denser and geometrically thinner outer molecular shell (traced most clearly by near-IR H_2 emission), and about 10% of the mass in a geometrically thicker but optically thinner inner shell of partially-ionized atomic gas (traced by near-IR and optical emission species [Fe II] and [Ni II]). This double-shell structure was first proposed based on H_2 and [Fe II] structures seen in the first available long-slit near-IR spectra of the Homunculus [105], although subsequent long-slit spectra of the same lines with higher resolution provided a much more definitive picture [108].

The double-shell structure is verified by $8\text{--}25\ \mu\text{m}$ imaging on large ground based telescopes with sub-arcsecond resolution [123], revealing a thin outer shell of cool dust with a color temperature of 140 K, and a thicker inner shell of warmer dust at 200 K in the polar lobes (Fig. 2). The thicker and warmer inner shell dominated previous mid-IR imaging at shorter wavelengths near $10\ \mu\text{m}$; Smith et al. [120] noted that the warm dust emitting at $10\text{--}12\ \mu\text{m}$ was $\sim 10\%$ less extended than the scattered light seen at visual and near-IR wavelengths, but did not articulate the nature of the double-shell structure. Fits to the IR SED imply that the outer 140 K shell contains about $11\ M_\odot$ of material, while the inner 200 K shell has only $1.5\ M_\odot$ [123].⁴

The effects of this double-shell structure are also clearly seen in UV echelle spectra obtained with STIS, tracing absorption along our line of sight to the central star. These spectra show narrow absorption lines from Fe I and diatomic molecules in the thin outer shell at $-530\ \text{km s}^{-1}$, and a more clumpy and broader distribution of absorption lines from singly-ionized metals at slower blueshifted speeds [49, 50, 83, 139]. For the thin outer shell, these same studies suggest that the gas temperature is $\sim 760\ \text{K}$, significantly warmer than the 140 K dust in the same location [123].

The double-shell structure is explained quantitatively in model calculations of the nebula’s ionization structure [113]. The inner shell is a warm (neutral-H) photodissociation region where metals like Fe and Ni are singly ionized by strong Balmer continuum radiation, while the outer thin and cool molecular shell exists where a thin layer of H_2 has absorbed much of the radiation in the Lyman-Werner bands. The required neutral H densities are roughly $10^{5.5}\ \text{cm}^{-3}$ in the inner shell (or more if the material is clumpy), and $(0.5\text{--}1)\times 10^7\ \text{cm}^{-3}$ in the outer shell in order to al-

⁴ Pantin & Le Mignant [92] proposed an “onion-like” structure for the polar lobes, with a smaller bubble inside a larger one. This structure was not verified in mid-IR images with higher resolution, and their proposed structure was not the double-shell structure described here.

low H_2 to survive and for Fe^+ to recombine to Fe^0 [113]. UV absorption features also suggest densities of 10^7 cm^{-3} in the thin outer molecular shell along our line of sight [49]. With densities this high, the observed volume of the cool shell would indicate high masses for the Homunculus of $\sim 20 M_\odot$ [108, 113].

What gives rise to this double-shell structure? On the one hand, the presence of near-IR H_2 and [Fe II] emission features remind one of warm shocked gas [110], in two zones behind the forward and reverse shocks, respectively. This would be somewhat misleading, however: comparing radiative energy heating to shock heating indicates that radiative heating dominates the energy balance by a factor of 250 or more [113]. Thus, the near-IR lines in the Homunculus do not trace current shock excitation as in a supernova remnant, for example, but instead trace different zones of ionization in a dense photodissociation region [113]. In near-IR lines of H_2 and [Fe II], this double-shell structure of the Homunculus is qualitatively identical to that seen in the planetary nebula M 2-9 [56, 118], where UV excitation is implied by the H_2 line ratios. If the density structure was imprinted by a shock, that shock interaction must have happened long ago [108]. Further work on this is needed.

Another unsolved issue is the origin of the clumpy, mottled structure apparent on the surfaces of the polar lobes. The true nature of the dark lanes vs. bright clumps, and of the obvious “hole” at the polar axis in the SE lobe have been topics of debate because different wavelengths or different techniques (imaging, spectroscopy, polarimetry) yield conflicting answers [80, 120, 123, 108, 102]. Recent spectra of H_2 have shown that the “hole” really is an absence of material [108], and IFU spectra of [Fe II] emission confirm its presence in the inner shell of the SE lobe as well as the receding NW polar lobe [134]. The nature of the cells and dark lanes remains an open question, however, and the answer potentially holds important clues to whether they originated in Rayleigh-Taylor instabilities, thermal instabilities, convective cells, or porosity [19, 120, 108, 89].

4.4 What Caused the Bipolar Shape?

Most theoretical work on the Homunculus has attempted to answer this question. The answer, which is not yet clear, is likely to be intimately connected to the cause of the Great Eruption, the star’s behavior before and after, and the potential roles of rotation and/or binarity in the system.

In some early models, the bipolar form of the Homunculus was said to arise from the interaction of winds of differing speed and density, shaping the outflow after ejection [38, 31, 66]. These borrowed from models for the ring and bipolar nebula of SN 1987A and planetary nebulae [9, 68, 37, 36]. The key requirement was a pre-existing, slow and dense equatorial disk or torus to pinch the waist of the bipolar structure. Observations, however, then showed that the equatorial skirt is no older than the polar lobes and some parts are younger [111, 81, 25]. We now know that there is not enough material near the equator to shape the overall morphology; instead, most of the mass is located at high latitudes in the polar lobes [108].

The next models to explain the morphology assumed that “intrinsic” shaping mechanisms had occurred in the ejection process. Acknowledging the apparent absence of any pre-existing “doughnut,” Frank et al. [39] suggested that the wind during the Great Eruption was fast and highly aspherical. This hypothesis was extended to the shaping of the Little Homunculus as well [45, 46]. While they yield bipolar nebulae resembling the Homunculus, these hydrodynamic models did not explain why the eruption wind was aspherical to begin with.

Smith et al. [124] showed that η Car’s present-day wind is in fact bipolar with more mass and higher speeds at the poles, and noted that if the present-day wind were given a mass-loss rate 1000 times stronger, it would look like the ballistically expanding Homunculus. IR observations [105, 108, 123] also showed that the shape of the lobes approximately agrees with what one expects for the latitudinal variation in escape speed on the surface of a rotating star, that more mass is located at the poles of the Homunculus, and that the thickness of the lobes compared to their radius is the same as the duration of the eruption divided by its age. The intrinsic bipolar mass ejection must presumably then be related to either rotation or to a companion star (or rotation induced by a companion star). In the context of aspherical line-driven winds, Owocki and coworkers [86, 87, 88] proposed that gravity darkening and velocity-dependent forces on a rotating star inhibit equatorial mass loss and *enhance the mass loss toward the poles*. Thus it was suggested that the Homunculus lobes arose from a bipolar continuum-driven wind with a higher polar mass-loss rate because of the latitudinal variation in escape speed [84, 85, 86, 67, 32]. This would require an enhanced wind for a brief time during the eruption, ejected directly from the surface of a rotating luminous star.

An intrinsically bipolar wind from a rotating star has several advantages over a pre-existing torus that pinches the waist, but there was still no explanation for the origin of the thin equatorial skirt described in §7 below. Smith & Townsend [117] noted that since disk-inhibition mechanisms arise because of velocity-dependent forces in a line-driven wind [87], a wind-compressed disk [8] could still be created in a continuum-driven wind. In that case the disk is formed by hyperbolic orbits crossing the equator after being launched from the surface of a rotating star, while the enhanced polar mass flux arises because of gravity darkening. Smith & Townsend showed that one can thereby account for both the shape of the polar lobes and a thin fast equatorial ejecta skirt.

In all the models mentioned so far, mass ejection by the primary star is the principle agent for shaping the nebula. (This includes a scenario where the rotating primary has increased angular momentum through interaction with a nearby companion [124]). Binary models have also been proposed to explain the bipolar shape. Soker [128, 129, 130, 131] advocates an analytic accretion model, where a close companion star in a binary system accretes matter from the primary wind through Bondi-Hoyle accretion, and then launches bipolar jets or collimated winds that shape the polar lobes. Alternatively, the idea of a binary merger (i.e. a merger of a close binary in a hierarchical triple system) has been suggested more than once to explain the Great Eruption and the origin of the bipolar nebula [40, 60, 79], but it

is difficult to understand the formation of the thin disk or the occurrence of previous giant eruptions in this type of scenario.

5 DUST, MOLECULES AND CHEMISTRY

By virtue of its phenomenal IR luminosity, the Homunculus has long been appreciated as a unique laboratory for the study of dust formation and survival in harsh conditions. The grains in the Homunculus are unusual compared to grains in the ISM and AGB stars in two important ways:

(1) They seem to be unusually large, $a \sim 1 \mu\text{m}$ or more, based on the following clues. The grains are near equilibrium blackbody temperatures [113, 123, 120, 51, 76, 77], their UV-to-IR extinction ratio is extraordinarily gray [98, 99, 5, 149, 53, 54], and they scatter efficiently even at $\sim 2 \mu\text{m}$ [112]. (Polarization properties of the nebula indicate that some small grains are also present [102].)

(2) They may have unusual composition, probably as a result of C and O depletion in the ejecta. While η Car shows what appears to be a strong $9.7 \mu\text{m}$ silicate feature, it is unusually broad and shifted to longer wavelengths. This has prompted suggestions that alternative grain mineralogy such as corundum (Al_2O_3) and olivine (MgFeSiO_4) might be present [75, 12]. In particular, Chesneau et al. [12] demonstrated that a combination of olivine and corundum can account for the observed shape of the spatially dependent “silicate” feature in the core of the Homunculus. The unusual composition of the grains may suggest that current mass estimates of the Homunculus of $10\text{--}15 M_\odot$ may be underestimates [26] (see above for other reasons why the mass estimates are conservative).

Our understanding of how these large and unusual grains nucleated rapidly and survived in the outflow of the Great Eruption is far from complete, and the puzzle deserves further investigation both theoretically and observationally. An additional mystery concerns the fact that gas-phase Fe has basically solar abundance in such a dusty region as the Homunculus [113]. Since we know when the material was ejected and when the dust formed from the historical record, and η Car is bright enough in the IR to provide high-quality data today, the Homunculus is a rare and valuable laboratory to address these questions.

In addition to unusual dust grains, the Homunculus harbors a surprisingly large mass of molecular gas, less than 0.1 pc from one of the most luminous hot supergiants known (i.e., η Car itself). Molecules were first discovered there via near-IR H_2 emission lines [110, 105], and were later shown to reside in the cool outer skin of each polar lobe [105, 108]. Given the presence of molecular hydrogen in a presumably nitrogen-rich environment, one might expect species like NH_3 , which indeed was the first polyatomic molecule detected in the Homunculus [119]. This was also the first detection of a polyatomic molecule around any LBV. UV absorption studies with STIS have revealed diatomic molecules such as CH and OH in the thin outer shell [139]. These UV absorption observations and radio studies have found no evidence for CO, presumably because most CNO in η Car’s ejecta is N rather than

C and O. While the outer ejecta and the inner Wiegelt Knots are known to be N-rich from their atomic emission-line spectra [22, 23, 115], the presence of ammonia gives our first reliable verification that the Homunculus too is N-rich [119]. The formation and survival of these molecules is far from understood, and more theoretical work on the molecular chemistry of the Homunculus would be useful [35].

6 THE LITTLE HOMUNCULUS

The Little Homunculus (LH) is a smaller bipolar nebula nested inside the main Homunculus, oriented along the same bipolar axis [63]. It is a relatively new addition to η Car’s family of known morphological features. The LH was briefly called the “integral-sign filament” (referring to the shape of its emission lines in *HST*/STIS spectrograms) and the “Matryoshka Nebula” [48, 62].

Its discovery by Ishibashi et al. was based on its Doppler-shift morphology in visual-wavelength spectra [63]; bright reflection nebulosity and extinction in the Homunculus make its structure very difficult to perceive in visual-wavelength images. The LH’s 3-D structure is best seen in near-IR emission lines of [Fe II], because these lines are bright and they can penetrate the foreground dust screen [105, 107]. This structure is clearly evident in Figure 3. The LH spans 4–5'' along the polar axis of the Homunculus [107]. It does not align with any features in visual scattered light, nor does it match the inner IR torus [107]. Since it was not detected at 10–20 μm , it probably does not contain a substantial amount of dust [123].

It does, however, match up quite well with the “Purple Haze” [126, 80] and the inner radio continuum nebula [29]. Smith [107] proposed that periodic and direction-dependent UV illumination of the LH is responsible for the extended radio continuum nebula and its associated changes through the 5.5 yr cycle. This could offer a powerful test of models for the 5.5 yr variability. Because it is seen in the radio continuum, the LH apparently absorbs whatever last remaining ionizing photons escape the dense wind of the central system.

Most indications suggest that the LH was ejected during η Car’s 1890 eruption. The LH has an expansion speed of 300 km s^{-1} at the poles and slower values at lower latitudes, with an expansion speed of $\sim 140 \text{ km s}^{-1}$ along our line of sight [107]. Thus, the LH is responsible for the -146 km s^{-1} absorption feature seen in high resolution UV spectra [49]. Walborn & Liller [144] noted blueshifted absorption features around 200 km s^{-1} in the spectrum observed during the 1890 event, making this association seem plausible. Nebular kinematics [107] and proper motions in STIS spectra [61] both imply an ejection date around 1910, but this assumes constant linear expansion. The LH’s polar expansion speed of 300 km s^{-1} is much slower than the 500–600 km s^{-1} stellar wind of η Car that pushes behind it, and Smith [107] showed that the LH would indeed be accelerated to its present value if it had been ejected in 1890, and that this acceleration leads us to infer an incorrect and more recent ejection date. The same may be true for the kinematics of the Wiegelt knots [125]. Smith [107] proposed that the Wiegelt knots are simply

the equatorial pinched waist of the LH, analogous to the IR torus of the larger Homunculus (see below). See also the chapter by Weigelt and Strauss on the inner ejecta in this volume.

Estimates of densities in the LH range from a few times 10^4 cm^{-3} [105] to 10^6 or even 10^7 cm^{-3} [63]. Combining the observed 3-D volume of the LH with an uncertain ionization fraction, the mass is estimated as $0.1 M_{\odot}$ [107], which is in rough agreement with other estimates based on upper limits to the dust mass and the kinematics. The kinetic energy of the 1890 event is then roughly $10^{46.9} \text{ erg}$ [107]. Given that the mass and kinetic energy of the 1890 event were orders of magnitude less than the Great Eruption [123], the fact that the two mass ejections shared the same basic geometry is thought provoking, to say the least. From a similar study of infrared [Fe II] emission from P Cygni's shell, Smith & Hartigan [114] concluded that the 1600 AD giant eruption of P Cygni was nearly identical to the 1890 lesser eruption of η Car in terms of its ejected mass, speed, and kinetic energy, although it was not bipolar. (See the chapter on the outer ejecta and other LBV-associated nebulae by Weis, this volume.)

7 EQUATORIAL STRUCTURES

7.1 The Equatorial Skirt

While bipolar lobes often occur in planetary nebulae and other astronomical objects, the ragged debris disk in η Carinae's equatorial plane is an uncommon and somewhat mysterious sight [19]. This equatorial "skirt" or "debris", as it is sometimes called to distinguish it from a smooth (and especially a Keplerian) disk, was first seen in high-resolution ground-based images [30]. Images with *HST* showed more detail in the radial streaks and other features [33, 19, 24, 80]. Images alone were inadequate, however, because some "equatorial features" later proved illusory.⁵ The geometrical thinness, planar form, and velocity structure of the skirt were especially apparent in *HST* spectral data [25], and Doppler velocities remain necessary to establish whether a feature is equatorial or not.

Though prominent in scattered-light images with brightness comparable to the polar lobes, the equatorial skirt is not seen clearly in thermal-IR maps [51, 120, 123, 93], suggesting that it contains little mass or that it is not heated efficiently. If the dust were cooler and substantially massive, however, one would expect the equatorial features to become more prominent at longer wavelengths or to cause severe extinction, but they are as hard to see at $25 \mu\text{m}$ as at $10 \mu\text{m}$ [123]. Smith et al. [123] have discussed the illumination of the equatorial ejecta in detail.

⁵ For instance, a bright fan-shaped structure $4''$ northwest of the star was often cited in the 1990s as an especially obvious equatorial feature. But Doppler velocities and IR measurements show that it is really a less-obscured patch of the NW polar lobe, despite appearances [25, 120, 123].

The age of the equatorial ejecta inspired a lively debate which is still not entirely settled [16, 111, 15, 81]. Proper motions at low spatial resolution with a time baseline of 50 years yielded an ejection date around 1885 for the equatorial features, suggesting that they came from the 1890 event [111]. Gaviola noted hints toward the same conclusion [41, 95]. Doppler velocities indicate post-1860 material in the skirt [19, 24, 25, 105, 107] and in the roughly-equatorial Weigelt Knots closer to the star [24, 28, 125, 147]. Proper motions measured in high-resolution *HST* data [15, 81], however, suggested that the skirt features were older, perhaps coeval with the Homunculus. Subsequent spectra showed emission lines in the equatorial material with *both* ages [25]. Thus, the resolution of the disagreement may be that the early blue plates (1945) and color slides (1972) were contaminated by line emission from younger diffuse gas originating in the 1890 event, whereas the small clumps measured in *HST* images were dust condensations tracing most of the mass. At least one of the features overlapped with the “Purple Haze” [126], a region of line emission that may be partly due to the younger Little Homunculus.

Only two models so far have attempted to explain the simultaneous origin of the polar lobes and this equatorial skirt, and in both cases the origin of the asymmetry was an inherently aspherical ejection by the star. Matt & Balick [70] presented a magnetohydrodynamic model for the present-day bipolar wind and disk, and conjectured that if this occurred at much higher mass-loss rate it may also explain the Homunculus. Smith & Townsend [117] presented a model of ejection from the surface of a rotating star that would produce a structure like the skirt via a compressed disk, along with the polar lobes. This type of mechanism is intuitively appealing because the required “splashing” at the equator may partly account for the ragged streaked appearance of the skirt [19, 24].

Some prominent features in the skirt share apparent connections to more distant and perplexing features in the outer nebulosity. For instance, the bright equatorial structure located $\sim 4''$ north-east of the star seems to connect to a nebular feature, sometimes termed the NN Condensation, north-east “jet”, or “NN jet” [143, ?, 73]. This structure extends radially in the same direction, driving an apparent bow-shock structure in the outer ejecta that is seen in nebular emission-line images [71, 73, 80]. Similarly, the streaked features in the skirt located west of the star appear to connect to the S Condensation. These perceived connections may be due to either common hydrodynamic flows or illusions caused by beams of starlight escaping in preferred directions, or both. These collimated protrusions⁶ in the equatorial plane have few parallels in astrophysical objects. These and additional structures in the outer ejecta are discussed further in the chapter by Weis.

⁶ One hesitates to call them “jets”, as they lack evidence of being steady collimated flows, but appear to have resulted from episodic mass ejections instead (e.g., [71]).

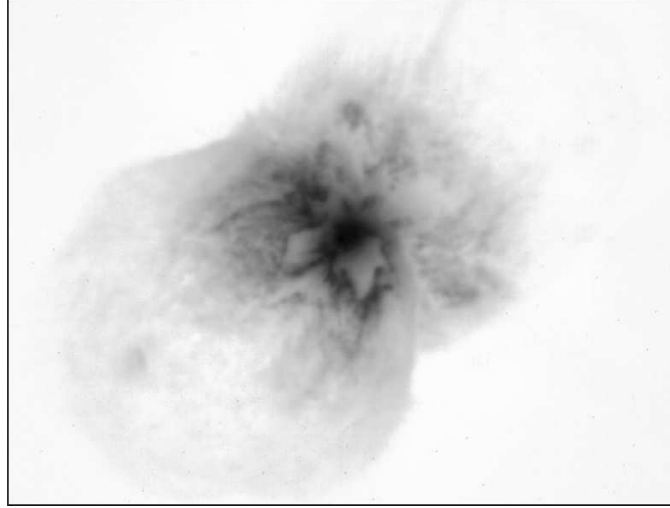


Fig. 4 A near-IR adaptive-optics image of the core of the Homunculus obtained with the VLT. This figure was prepared by the author from a *K*-band image kindly provided by O. Chesneau (see [12]).

7.2 The Obscured Inner Torus

As noted earlier, IR imaging during the 1970s–1990s revealed a complex, multi-peaked structure in the core of the Homunculus. Several near-IR and mid-IR studies with 2–4-m class telescopes, each of which improved on previous work, unveiled these inner structures at high resolution, most often interpreted as some variation of a dusty torus [51, 103, 94, 34, 120, 78, 93, 112, 55]. Access to mid-IR imaging on 6–8 m class telescopes improved our view of the torus [122], and we now have stunning adaptive optics images in the near-IR (Fig. 4) obtained with the VLT [12].

Like the larger equatorial skirt, this compact and complex structure has sparked interesting debates. Morris et al. [78] proposed that this structure was a pre-existing $15 M_{\odot}$ torus, including the 110 K dust that dominated the far-IR flux, and was the agent responsible for pinching the waist of the Homunculus. Davidson & Smith [21] argued against this interpretation, and pointed out that the torus was actually quite warm. Hony et al. [55] proposed that the inner structure was a pair of polar rings like those around SN 1987A, and that the polar axis of the binary system had precessed by $37\text{--}58^{\circ}$ caused by a close interaction of a triple system. Smith et al. [122] presented higher resolution images showing that these rings were an artifact of lower spatial resolution, resembling a fragmented torus instead. Chesneau et al. [12] presented even higher-resolution images showing surprisingly complex structure (Fig. 4), and proposed that these unprecedented features were part of an inner bipolar nebula that they named the “butterfly nebula”.

Examination of narrow H_2 velocities in near-IR long-slit echelle spectra showed that the dusty features in question were in the mid-plane of the Homunculus where

the two polar lobes meet at the pinched waist of the nebula, and were not related to polar features of the Little Homunculus [107, 108]. The expected dust temperatures at this location agree with the observed warm color temperatures of the dust of 250–400 K [123]. The strange and irregularly corrugated structures seen in the VLT images [12] probably result from the strong post-eruption wind of η Car pushing out the relatively low density regions in between clumps in the torus [122]. In some cases, perhaps these protrusions have broken all the way through in the mid plane, allowing the stars visual light to escape to large radii, producing radial streaks seen in images of reflected light. This provides only a partial explanation for outer features like the NN jet and the S Condensation, which still evade our understanding. See relevant chapters this volume by Weis and by Weigelt and Strauss.

The clumpy torus seen in near- and mid-IR images has no counterpart in visual-wavelength images in scattered light, but it can be seen by virtue of its emission-line variability caused by ionization changes during the 5.5 yr cycle [121], and it can be recognized by its Doppler shifted narrow line emission in long-slit STIS spectra of the inner Homunculus [47].

8 SUMMARY: FAST FACTS

The Homunculus of η Car is a spectacular and complex object that is a rich laboratory for studying many phenomena associated with ISM processes and the physics of stellar mass loss. It is in its scattered starlight at visual and near-IR wavelengths, allowing us to see the star from multiple directions [124], but it also has intrinsic emission features that tell us about the kinematics and excitation of the nebula [53, 25, 108, 113]. Its intrinsic spectrum is that of a low-ionization warm photodissociation region, but with peculiar gas and dust abundances. Extended emission has been detected at all wavelengths from scattered X-rays [13], the UV [125], visual and near-IR wavelengths, thermal-IR, and even low-level radio continuum emission from the polar lobes [29]. It is rivaled by few other objects in the sky, but its complexity often defies the simplest interpretation. Our understanding of the Homunculus will no-doubt continue to improve, but here I list current best estimates for several observed properties of the nebula:

- Proper motions measured with post-refurbishment *HST* images give an ejection date for the Homunculus of 1847 (± 4 –6 yr) [81]. This is consistent with the 1843 eruption peak within the uncertainty, but hints that there may have been some post-ejection acceleration.
- The total IR luminosity integrated from 2–200 μm is $4.3 \times 10^6 L_{\odot}$ [123]. The total stellar luminosity is 10–20% higher than this, since that much UV/visual light escapes.
- The total mass of the Homunculus (gas + dust) is at least 12–15 M_{\odot} [123, 78, 113], but could be substantially more as noted above. The total kinetic energy is then at least $10^{49.7}$ erg [123].

- The shape of the polar lobes is traced best by near-IR H_2 emission [108] and is shown in Figure 3. Smith [108] also gives the expansion speed, mass, and kinetic energy as a function of latitude. Most of the mass and kinetic energy is at high latitudes.
- The heliocentric distance to the Homunculus, derived from its proper motion and observed Doppler shifts assuming axisymmetry, is 2.3 ± 0.05 kpc [74, 25, 105, 108].
- The inclination angle of the Homunculus (the angle that the polar axis is tilted from the line-of-sight) is $i = 42^\circ \pm 1^\circ$ [25, 108].
- The systemic velocity of η Car is $-8.1(\pm 1) \text{ km s}^{-1}$ heliocentric, or $-19.7(\pm 1) \text{ km s}^{-1}$ LSR, measured from narrow H_2 lines [106].
- The Homunculus has a well-defined double-shell structure. The thin outer shell has about 90% of the total mass, is primarily molecular gas, Fe is neutral, the particle density is $\sim 10^7 \text{ cm}^{-3}$, and the dust temperature is about 140 K. The inner shell is thicker and less massive, the dust is warmer at about 200 K, metals like Fe and Ni are singly ionized, and H is mostly neutral.
- The dust grains that dominate thermal emission and excitation are large, with $a \simeq 1 \mu\text{m}$. Judging by the $10 \mu\text{m}$ emission feature, the chemical makeup of the dust appears to be unusual compared to other evolved stars, with significant amounts of corundum and olivine.
- The detection of NH_3 and lack of CO verifies that the neutral/molecular Homunculus is N-rich like the outer ejecta and Weigelt knots [119]. The molecules that have been detected so far are H_2 [105], CH and OH [139], and NH_3 [119]. Verner et al. suggest that CH^+ , CH_2^+ , CH_2 , and NH may also be detectable. One might also expect to find N_2H^+ [119]. In other words, the Homunculus is a valuable laboratory for studying N-rich molecular chemistry.
- Most of the dense clumpy structures in the equatorial skirt seen in optical images were ejected at the same time as the polar lobes. There is also younger material from the 1890 eruption intermixed with these equatorial ejecta, seen mainly in emission lines. The equatorial skirt is *not* a pre-existing disk that pinched the waist of the nebula.
- Infrared images show a bright IR torus inside the Homunculus that is not seen in visual-wavelength images. It is bright in the IR because it contains some of the warmest dust in the Homunculus, where the thin walls of the two polar lobes meet at the equator. The mass in this torus is not nearly enough to have pinched the waist of the Homunculus.

9 THE FUTURE FOR THE HOMUNCULUS

Eta Carinae is among the most bizarre extended objects in the sky, with some of the most spectacularly complex and puzzling circumstellar structures known. It is wise to keep this in perspective, however, remembering that many of the reasons the Homunculus seems so peculiar arise *because it is so young*. It is young enough that

it is still in free expansion, and so the observed geometry still bears the imprint of the initial ejection – before its signature is erased by deceleration from the surrounding medium. This makes η Car unique among massive stars, and this is why it is such a valuable tool for constraining the physics of episodic mass loss from massive stars. It is therefore instructive to end by briefly considering the future fate of the Homunculus:

In another 500–1000 years, the Homunculus will have expanded to ~ 5 times its current size, and will plow into the outer ejecta. Its very clean bipolar and thin disk geometry will probably be diluted or erased. It will no longer obscure the central star (and will therefore be harder to observe), and it will not be one of the brightest 10–20 μm objects in the sky because the dust will absorb a smaller fraction of the total luminosity and will be much cooler. At lower densities it will probably be largely ionized (if not by η Car, then by the remaining ~ 60 O-type stars in the Carina nebula), and the thin outer molecular shell will probably not survive.

In other words, it will probably appear as a fairly ill-defined, hollow ellipsoidal ionized gas shell with unclear kinematics, much like η Car’s current outer ejecta from a previous eruption or the nebula around AG Car [132, 104, 141]. In context, then, the Homunculus is perhaps not so bizarre after all, since shell nebulae with masses of $\sim 10 M_{\odot}$ are not unusual for LBVs with luminosities above $10^6 L_{\odot}$ [116]. This epitaph underscores how lucky we are to observe the Homunculus in our lifetimes with available technology at an optimal time when $\tau=1$ throughout much of the nebula. Until the distant (or not so distant?) future when fuel has been exhausted in the star’s core, the Homunculus will continue to disperse, leaving the star unobscured when it explodes...unless another giant eruption happens first.

Acknowledgements I am indebted to numerous people with whom I have collaborated on studies of the Homunculus and discussed related topics, especially Kris Davidson, Gary Ferland, Bob Gehrz, John Hillier, Jon Morse, Stan Owocki, and Rich Townsend.

References

1. Aitken, D.K., & Jones, B. 1975, MNRAS, 172, 141-147. “The Infrared Spectrum and Structure of Eta Carinae.”
2. Aitken, D.K., Smith, C.H., Moore, T.J.T., Roche, P.F. 1995, MNRAS, 273, 359-366. “Mid-Infrared Studies of Eta Carinae - II. Polarimetric Imaging at 12.5 micron and the Magnetic Field Structure.”
3. Allen, D.A. 1989, MNRAS, 241, 195-207. “The Hollow, Clumpy Outflow Around Eta Carinae.”
4. Allen, D.A., & Hillier, D.J. 1993, PASA, 10, 338-341. “The Shape of the Homunculus Nebula Around Eta Carinae.”
5. Andriesse, C.D., Donn, B.D., & Viotti, R. 1978, MNRAS, 185, 771-788. “The Condensation of Dust Around Eta Carinae.”
6. Apruzese, J.P. 1975, ApJ, 196, 753-760. “Radiative Transfer in Spherical Circumstellar Dust Envelopes. II. Is the Infrared Continuum of Eta Carinae Produced by Thermal Dust Emission?”

7. Bensammar, S., Letourneur, N., Perrier, F., Friedjung, M., & Viotti, R. 1985, *A&A*, 146, L1-L2. "Multiplex Imagery of the Infrared Core of Eta Carinae."
8. Bjorkmann, J.F., & Cassinelli, J.P. 1993, *ApJ*, 409, 429-449. "Equatorial Disk Formation Around Rotating Stars due to Ram Pressure Confinement by the Stellar Wind."
9. Blondin, J., & Lundqvist, P. 1993, *ApJ*, 405, 337-352. "Formation of the Circumstellar Shell Around SN 1987A."
10. Briggs, G.R., & Aitken, D.K. 1985, *PASA*, 6, 145-147. "Middle Infrared Spectropolarimetry of Eta Carinae."
11. Chelli, A., Perrier, C., & Biraud, Y.G. 1983, *A&A*, 117, 199-204. "One-Dimensional High Resolution Image Reconstruction on Eta Carinae at 4.6 micron with Speckle Data."
12. Chesneau, O., et al. 2005, *A&A*, 435, 1043-1061. "The Sub-arcsecond Dusty Environment of Eta Carinae."
13. Corcoran, M.F., et al. 2004, *ApJ*, 613, 381-386. "Waiting in the Wings: Reflected X-ray Emission from the Homunculus Nebula."
14. Cox, P., et al. 1995, *A&A*, 297, 168-174. "Millimeter Emission of Eta Carinae and its Surroundings."
15. Currie, D.G., & Dowling, D.M. 1999, in *ASP Conf. Ser. 179, Eta Carinae at the Millenium*, ed. J.A. Morse, R.M. Humphreys, & A. Damineli (San Francisco: ASP), 72-82. "Astrometric Motion and Doppler Velocity."
16. Currie, D.G., et al. 1996a, *AJ*, 112, 1115-1127. "Astrometric Analysis of the Homunculus of Eta Carinae with the Hubble Space Telescope."
17. Currie, D.G., et al. 1996b, in *The Role of Dust in the Formation of Stars*, H.U. Käufl & R. Siebenmorgen, eds., (Springer: Berlin), 89-94. "3-D Structure of the Bipolar Dust Shell of Eta Carinae."
18. Davidson, K. 1971, *MNRAS*, 154, 415-427. "On the Nature of Eta Carinae."
19. Davidson, K., & Humphreys, R.M. 1997, *ARA&A*, 35, 1. "Eta Carinae and its Environment."
20. Davidson, K., & Ruiz, M.T. 1975, *ApJ*, 202, 421-424. "Scattering by Dust and the Photographic Appearance of Eta Carinae."
21. Davidson, K., & Smith, N. 2000, *Nature*, 405, 532. "A Massive Cool Dust Torus Around Eta Carinae?"
22. Davidson, K., Dufour, R.J., Walborn, N.R., & Gull, T.R. 1986, *ApH*, 305, 867-879. "Ultraviolet and Visual Wavelength Spectroscopy of Gas Around Eta Carinae."
23. Davidson, K., Ebbets, D., Weigelt, G., Humphreys, R.M., Hajian, A., Walborn, N.R., & Rosa, M. 1995, *AJ*, 109, 1784-1796. "HST/FOS Spectroscopy of Eta Carinae: The Star Itself, and Ejecta Within 0.3 Arcsec."
24. Davidson, K., Ebbets, D., Johansson, S., Morse, J.A., Hamann, F.W., Balick, B., Humphreys, R.M., Weigelt, G., & Frank, A. 1997, *AJ*, 113, 335-345. "HST/GHRS Observations of the Compact Slow Ejecta of Eta Carinae."
25. Davidson, K., Smith, N., Gull, T.R., Ishibashi, K., & Hillier, D.J. 2001, *AJ*, 121, 1569-1577. "The Shape and Orientation of the Homunculus Nebula Based on Spectroscopic Velocities."
26. de Koter, A., Min, M., van Boekel, R., & Chesneau, O. 2005, in *ASP Conf. Ser. 332, The Fate of the Most Massive Stars*, ed. R. Humphreys, & K. Stanek (San Francisco: ASP), 313-316. "The Solid-State Composition and Mass of the Homunculus of Eta Carinae."
27. de Vaucouleurs, G., & Eggen, O.C. 1952, *PASP*, 64, 185-190. "The Brightening of Eta Carinae."
28. Dorland, B.N., Currie, D.G., & Hajian, A.R. 2004, *AJ*, 127, 1052-1058. "Did Eta Carinae's Weigelt Blobs Originate Circa 1941?"
29. Duncan, R.A., White, S.M., & Lim, J. 1997, *MNRAS*, 290, 680-688. "Evolution of the Radio Outburst from the Supermassive Star Eta Carinae from 1992 to 1996."
30. Duschl, W.J., Hofman, K.H., Rigaut, F., & Weigelt, G. 1995, *Rev. Mex. AA, Ser. Conf.*, 2, 17. "Morphology and Kinematics of Eta Carinae."
31. Dwarkadas, V.V., & Balick, B. 1998, *AJ*, 116, 829-839. "On the Formation of the Homunculus Nebula Around Eta Carinae."
32. Dwarkadas, V.V., & Owocki, S.P. 2002, *ApJ*, 581, 1337-1343. "Radiatively Driven Winds and the Shaping of Bipolar Luminous Blue Variable Nebulae."

33. Ebbets, D., Garner, H., White, R., Davidson, K., Malumuth, E., & Walborn, N. 1994, in: *Circumstellar Media in Late Stages of Stellar Evolution*. 34th Herstmonceux Conf., Clegg, R.E.S., Stevens, I.R., Meikle, W.P.S. (eds.) (Cambridge: Cambridge University Press), 95–97. “HST images of Eta Carinae.”
34. Falcke, H., Davidson, K., Hofmann, K.H., & Weigelt, G. 1996, *A&A*, 306, L17-L20. “Speckly-Masking Imaging Polarimetry of Eta Carinae: Evidence for an Equatorial Disk.”
35. Ferland, G.J., Abel, N., Davidson, K., & Smith, N. 2005, in *ASP Conf. Ser. 332, The Fate of the Most Massive Stars*, ed. R. Humphreys, & K. Stanek (San Francisco: ASP), 294-301. “Physical Conditions in the Homunculus.”
36. Frank, A. 1999, *New. Astron. Rev.*, 43, 31-65. “Bipolar outflows and the evolution of stars.”
37. Frank, A., & Mellema, G. 1994, *ApJ*, 430, 800-813. “The radiation gas dynamics of planetary nebulae. IV. From the Owl to the Eskimo.”
38. Frank, A., Balick, B., & Davidson, K. 1995, *ApJ*, 441, L77-L80. “The Homunculus of Eta Carinae: An Interacting Stellar Winds Paradigm.”
39. Frank, A., Ryu, D., & Davidson, K. 1998, *ApJ*, 500, 291-301. “Where is the Doughnut? Luminous Blue Variable Bubbles and Aspherical Fast Winds.”
40. Gallagher, J.S. 1989, in *Physics of Luminous Blue Variables*, ed. K. Davidson, A.F.J. Moffat, & H.J.G.L.M. Lamers (Dordrecht: Kluwer), 185-194. “Close Binary Models for Luminous Blue Variable Stars.”
41. Gaviola, E. 1950, *ApJ*, 111, 408-413. “Eta Carinae. I. The Nebulosity.”
42. Gehrz, R.D., & Ney, E.P. 1972, *Sky & Telescope*, 44, 4-5. “The Core of Eta Carinae.”
43. Gehrz, R.D., Ney, E.P., Becklin, E.E., & Neugebauer, G. 1973, *Astroph. Lett.*, 13, 89-93. “The Infrared Spectrum and Angular Size of Eta Carinae.”
44. Gomez, H.L., Dunne, L., Eales, S.A., & Edmunds, M.G. 2006, *MNRAS*, 372, 1133-1139. “Submillimetre Emission from Eta Carinae.”
45. Gonzalez, R., de Gouveia Dal Pino, E.M., Raga, A.C., & Velazquez, P.F. 2004a, *ApJ*, 600, L59-L62. “Gasdynamical Simulations of the Large and Little Homunculus Nebulae of Eta Carinae.”
46. Gonzalez, R., de Gouveia Dal Pino, E.M., Raga, A.C., & Velazquez, P.F. 2004b, *ApJ*, 616, 976-987. “Numerical Modeling of Eta Carinae Bipolar Outflows.”
47. Gull, T.R., & Ishibashi, K. 2001, in *ASP Conf. Ser. 242, Eta Carinae & Other Mysterious Stars*, ed. T. Gull, S. Johansson, & K. Davidson (San Francisco: ASP), 59-70. “The Three-Dimensional and Time-Variant Structures of Ejecta Around Eta Carinae as Detected by the STIS.”
48. Gull, T.R., Ishibashi, K., Davidson, K., & the Cycle 7 STIS GTO Team 1999, in *ASP Conf. Ser. 179, Eta Carinae at the Millenium*, ed. J.A. Morse, R.M. Humphreys, & A. Damineli (San Francisco: ASP), 144-154. “First Observations of Eta Carinae with the Space Telescope Imaging Spectrograph.”
49. Gull, T.R., Viera, G., Bruhweiler, F., Nielsen, K.E., Verner, E., & Danks, A. 2005, *ApJ*, 620, 442-449. “The Absorption Spectrum of High-Density Stellar Ejecta in the Line of Sight to Eta Carinae.”
50. Gull, T.R., Viera Kober, G., & Nielsen, K.E. 2006, *ApJS*, 163, 173-183. “Eta Carinae Across the 2003.5 Minimum: The Character and Variability of the Ejecta Absorption in the Near-Ultraviolet.”
51. Hackwell, J.A., Gehrz, R.D., & Grasdalen, G.L. 1986, *ApJ*, 311, 380-399. “The Internal Structure of the Dust Shell of Eta Carinae Deduced from Six Channel 8-13 micron Mapping.”
52. Hillier, D.J. 1997, in *ASP Conf. Ser. 120, Luminous Blue Variables: Massive Stars in Transition*, ed. A. Nota & H.J.G.L.M. Lamers (San Francisco: ASP), 287-293. “Models for Eta Carinae.”
53. Hillier, D.J., & Allen, D.A. 1992, *A&A*, 262, 153-170. “A Spectroscopic Investigation of Eta Carinae and the Homunculus Nebula. I. Overview of the Spectra.”
54. Hillier, D.J., Davidson, K., Ishibashi, K., & Gull, T.R. 2001, *ApJ*, 553, 837-860. “On the Nature of the Central Source in Eta Carinae.”
55. Hony, S., et al. 2001, *A&A*, 377, L1-L4. “Discovery of a Double Ring in the Core of Eta Carinae.”

56. Hora, J.L., & Latter, W.B. 1994, *ApJ*, 437, 281-295. "The Near-Infrared Structure and Spectra of the Bipolar Nebulae M2-9 and AFGL 2688: The Role of Ultraviolet Pumping and Shocks in Molecular Hydrogen Excitation."
57. Humphreys, R.M., & Davidson, K. 1994, *PASP*, 106, 1025. "The Luminous Blue Variables: Astrophysical Geysers."
58. Humphreys, R.M., Davidson, K., & Koppelman, M. 2008, *AJ*, 135, 1249-1263. "The Early Spectra of Eta Carinae 1892 to 1941 and the Onset of its High Excitation Emission Spectrum."
59. Hyland, A.R., Robinson, G., Mitchell, R.M., Thomas, J.A., & Becklin, E.E. 1979, *ApJ*, 233, 145-153. "The Spectral and Spatial Distribution of Radiation from Eta Carinae. II. High-Resolution Infrared Maps of the Homunculus."
60. Iben, I. 1999, in *ASP Conf. Ser.* 179, *Eta Carinae at the Millenium*, ed. J.A. Morse, R.M. Humphreys, & A. Damineli (san Francisco: ASP), 367-372. "The Effects of Possible Binary and Tertiary Companions on the Behavior of Eta Carinae."
61. Ishibashi, K. 2005, in *ASP Conf. Ser.* 332, *The Fate of the Most Massive Stars*, ed. R. Humphreys, & K. Stanek (San Francisco: ASP), 131-136. "Historical Eruptions of Eta Carinae: Looking Through the Homunculus."
62. Ishibashi, K., Gull, T.R., & Davidson, K. 2001, in *ASP Conf. Ser.* 242, *Eta Carinae & Other Mysterious Stars*, ed. T. Gull, S. Johansson, & K. Davidson (San Francisco: ASP), 71-79. "The HST/STIS Mapping of the Eta Carinae Nebula."
63. Ishibashi, K., et al. 2003, *AJ*, 125, 3222-3236. "Discovery of a Little Homunculus Within the Homunculus Nebula of Eta Carinae."
64. Joyce, R.R. 1975, *PASP*, 87, 917-921. "The Infrared Spectrum of Eta Carinae: 3-14 microns."
65. Krishna Swamy, K.S. 1971, *Obs.*, 91, 120-123. "On the Infra-Red Radiation from Eta Carinae."
66. Langer, N., Garcia-Segura, G., & Mac Low, M.M. 1999, *ApJ*, 520, L49-L53. "Giant Outbursts of Luminous Blue Variables and the Formation of the Homunculus Nebula Around Eta Carinae."
67. Maeder, A., & Desjacques, V 2001, *A&A*, 372, L9-L12. "The shape of Eta Carinae and LBV Nebulae."
68. Martin, C.L., & Arnett, W.D. 1985, *ApJ*, 447, 378-390. "The Origin of the Rings around SN 1987A: an Evaluation of the Interacting-Winds Model."
69. Martin, J.C., Davidson, K., & Koppelman, M.D. 2006, *AJ*, 132, 2717-2728. "The Chrysalis Opens? Photometry from the Eta Carinae Hubble Space Telescope Treasury Project, 2002-2006."
70. Matt, S., & Balick, B. 2004, *ApJ*, 615, 921-933. "Simultaneous Production of Disk and Lobes: A Single-Wind MHD Model for the Eta Carinae Nebula."
71. Meaburn, J., Wolstencroft, R.D., & Walsh, J.R. 1987, *A&A*, 181, 333-342. "Echelle and Spectropolarimetric Observations of the Eta Carinae Nebulosity."
72. Meaburn, J., Walsh, J.R., & Wolstencroft, R.D. 1993, *A&A*, 268, 283-293. "The Outflowing Dust Around Eta Carinae."
73. Meaburn, J., Gehring, G., Walsh, J.R., Palmer, J.W., Lopez, J.A., Bryce, M., & Raga, A.C. 1993, *A&A*, 276, L21-L24. "An Episodic Jet from Eta Carinae."
74. Meaburn, J. 1999, In: *ASP Conf. Ser.* 179, *Eta Carinae at the Millennium*, ed. J.A. Morse, R.M. Humphreys, & A. Damineli, (San Francisco: ASP), 89-91. "An Updated Proper-Motion/Spectropolarimetric Distance to η Carinae."
75. Mitchell, R.M., & Robinson, G. 1978, *ApJ*, 220, 841-852. "The Spectral and Spatial Distribution of Radiation from Eta Carinae. I. A Spherical Dust Shell Model Approach."
76. Mitchell, R.M., & Robinson, G. 1986, *MNRAS*, 222, 347-355. "Grain Size and Geometrical Effects in the Eta Carinae Dust Shell."
77. Mitchell, R.M., Robinson, G., Hyland, A.R., & Jones, T.J. 1983, *ApJ*, 271, 133-142. "The Spectral and Spatial Distribution of Radiation from Eta Carinae. III. A High Resolution 2.2 micron Map and Morphological Considerations of the Evolutionary Status."
78. Morris, P.W., et al. 1999, *Nature*, 402, 502-504. "Discovery of a Massive Equatorial Torus in the Eta Carinae Stellar System."

79. Morris, T., & Podsiadlowski, P. 2006, MNRAS, 365, 2-10. "Anisotropic Mass Ejection in Binary Mergers."
80. Morse, J.A., Davidson, K., Bally, J., Ebbets, D., Balick, B., & Frank, A. 1998, AJ, 116, 2443-2461. "Hubble Space Telescope Wide Field PLanetary Camera 2 Observations of Eta Carinae."
81. Morse, J.A., Kellogg, J.R., Bally, J., Davidson, K., Balick, B., & Ebbets, D. 2001, ApJ, 548, L207-L211. "Hubble Space Telescope Proper-Motion Measurements of the Eta Carinae Nebula."
82. Neugebauer, G., & Westphal, J.A. 1968, ApJ, 152, L89-L94. "Infrared Observations of Eta Carinae."
83. Nielsen, K.E., Gull, T.R., & Viera Kober, G. 2005, ApJS, 157, 138-146. "The Ultraviolet Spectrum of Eta Carinae: Investigation of the Ejecta Absorption."
84. Owocki, S.P. 2003, in IAU Symp. 212, A Massive Star Odyssey: From Main Sequence to Supernova, ed. K. van der Hucht, A. Herrero, & C. Esteban (San Francisco: ASP), 281-290. "Instabilities in Massive Stars."
85. Owocki, S.P. 2005, in ASP Conf. Ser. 332, The Fate of the Most Massive Stars, ed. R. Humphreys, & K. Stanek (San Francisco: ASP), 169-179. "Radiatively Driven Stellar Winds and Aspherical Mass Loss."
86. Owocki, S.P., & Gayley, K.G. 1997, in ASP Conf. Ser. 120, Luminous Blue Variables: Massive Stars in Transition, ed. A. Nota & H.J.G.L.M. Lamers (San Francisco: ASP), 121-127. "The Physics of Stellar Winds Near the Eddington Limit."
87. Owocki, S.P., Cranmer, S.R., & Gayley, K. 1996, ApJ, 472, L115-L118. "Inhibition FO Wind Compressed Disk Formation by Nonradial Line-Forces in Rotating Hot-Star Winds."
88. Owocki, S.P., Cranmer, S.R., & Gayley, K. 1998, Ap&SS, 260, 149-159. "Mass Loss from Rotating Hot-stars: Inhibition of Wind Compressed Disks by Nonradial Line-Forces."
89. Owocki, S.P., Gayley, K.G., & Shaviv, N.J. 2004, ApJ, 616, 525-541. "A Porosity-Length Formalism for Photon-Tiring-limited Mass Loss from Stars above the Eddington Limit."
90. Pagel, B.E.J. 1969a, Nature, 221, 325-327. "Intrinsic Reddening of Eta Carinae."
91. Pagel, B.E.J. 1969b, Astrop. Lett., 4, 221-224. "Energy Budget for the Infrared Radiation from Eta Carinae."
92. Pantin, E., & Le Mignant, D. 2000, A&A, 355, 155-164. "17 micron Imaging of Eta Carinae: An Onion-Like Structure for the Lobes?"
93. Polomski, E., Telesco, C.M., Pina, R.K., & Fisher, R.S. 1999, AJ, 118, 2369-2377. "Complex Structure of Eta Carinae in the Mid-Infrared."
94. Rigaut, F., & Gehring, G. 1995, Rev. Mex. AA, Ser. Conf., 2, 27-35. "The Inner Core of Eta Carinae in the Near Infrared."
95. Ringuelet, A.E. 1958, Z. f. Astroph., 46, 276-278. "Note on the Nebulosity Around Eta Carinae."
96. Robinson, G., Hyland, A.R., & Thomas, J.A. 1973, MNRAS, 161, 281-292. "Observation and Interpretation of the Infra-Red Spectrum of Eta Carinae."
97. Robinson, G., Mitchell, R.M., Aitken, D.K., Briggs, G.P., & Roche, P.F. 1987, MNRAS, 227, 535-542. "Infrared Studies of Eta Carinae - I. Spectroscopy and a Composite Dust Model."
98. Rodgers, A.W. 1971, ApJ, 165, 665-667. "The Reddening of Eta Carinae."
99. Rodgers, A.W., & Searle 1967, MNRAS, 135, 99-119. "Spectrophotometry of the Object Eta Carinae."
100. Russel, R.W., et al. 1987, ApJ, 321, 937-942. "Airborne Spectrophotometry of Eta Carinae from 4.5 to 7.5 microns and a Model for Source Morphology."
101. Schulte-Ladbeck, R.E., et al. 1997, in ASP Conf. Ser. 120, Luminous Blue Variables: Massive Stars in Transition, ed. A. Nota & H.J.G.L.M. Lamers (San Francisco: ASP), 260-266. "The Structure of Eta Carinae's Homunculus from Imaging Polarimetry and Spectropolarimetry."
102. Schulte-Ladbeck, R.E., et al. 1999, AJ, 118, 1320-1337. "Hubble Space Telescope Imaging Polarimetry of Eta Carinae."

103. Smith, C.H., Aitken, D.K., Moore, T.J.T., Roche, P.F., Puetter, R.C., & Pina, R.K. 1995, MNRAS, 273, 354-358. "Mid-infrared Studies of Eta Carinae-I. Subarcsecond Imaging of 12.5 and 17 micron."
104. Smith, L.J., Stroud, M.P., Esteban, C., & Vilchez, M. 1997, MNRAS, 290, 265-275. "The AG Carinae Nebula: Abundant Evidence for a Red Supergiant Progenitor?"
105. Smith, N. 2002, MNRAS, 337, 1252-1268. "Dissecting the Homunculus Nebula Around Eta Carinae with Spatially Resolved Near-Infrared Spectroscopy."
106. Smith, N. 2004, MNRAS, 351, L15-L18. "The Systemic Velocity of Eta Carinae."
107. Smith, N. 2005, MNRAS, 357, 1330-1336. "Doppler Tomography of the Little Homunculus: High-Resolution Spectra of [Fe II] 16435 Around Eta Carinae."
108. Smith, N. 2006, ApJ, 644, 1151-1163. "The Structure of the Homunculus. I. Shape and Latitude Dependence from H₂ and [Fe II] Velocity Maps of Eta Carinae."
109. Smith, N., & Davidson, K. 2000, Nature, 405, 532. "A Massive Cool Dust Torus Around Eta Carinae?"
110. Smith, N., & Davidson, K. 2001, ApJ, 551, L101-L104. "The Shocking Near-Infrared Spectrum of the Homunculus Nebula Surrounding Eta Carinae."
111. Smith, N., & Gehrz, R.D. 1998, AJ, 116, 823-828. "Proper Motions in the Ejecta of Eta Carinae with a 50 Year Baseline."
112. Smith, N., & Gehrz, R.D. 2000, ApJ, 529, L99-L102. "Recent Changes in the Near-Infrared Structure of Eta Carinae."
113. Smith, N., & Ferland, G.J. 2007, ApJ, 655, 911-919. "The Structure of the Homunculus. II. Modeling the Physical Conditions in Eta Carinae's Molecular Shell."
114. Smith, N., & Hartigan, P. 2006, ApJ, 638, 1045-1055. "Infrared [Fe II] Emission from P Cygni's Nebula: Atomic Data, Mass, Kinematics, and the 1600 AD Outburst."
115. Smith, N., & Morse, J.A. 2004, ApJ, 605, 854-863. "Nitrogen and Oxygen Abundance Variations in the Outer Ejecta of Eta Carinae: Evidence for Recent Chemical Enrichment."
116. Smith, N., & Owocki, S.P. 2006, ApJ, 645, L45-L48. "On the Role of Continuum-Driven Eruptions in the Evolution of Very Massive Stars and Population III Stars."
117. Smith, N., & Townsend, R.H.D. 2007, ApJ, 666, 967-975. "The Structure of the Homunculus. III. Forming a Disk and Bipolar Lobes in a Rotating Surface Explosion."
118. Smith, N., Balick, B., & Gehrz, R.D. 2005, AJ, 130, 853-861. "Kinematic Structure of H₂ and [Fe II] in the Bipolar Planetary Nebula M2-9."
119. Smith, N., Brooks, K.J., Koribalski, B., & Bally, J. 2006, ApJ, 645, L41-L44. "Cleaning Up Eta Carinae: Detection of Ammonia in the Homunculus Nebula."
120. Smith, N., Gehrz, R.D., & Krautter, J. 1998, AJ, 116, 1332-1345. "The Infrared Morphology of Eta Carinae."
121. Smith, N., Morse, J.A., Davidson, K., & Humphreys, R.M. 2000, AJ, 120, 920-934. "Recent Changes in the Near-Ultraviolet and Optical Structure of Eta Carinae."
122. Smith, N., Gehrz, R.D., Hinz, P.M., Hoffmann, W.F., Mamajek, E.E., Meyer, M.R., & Hora, J.L. 2002, ApJ, 567, L77-L80. "A Disrupted Circumstellar Torus Inside Eta Carinae's Homunculus Nebula."
123. Smith, N., Gehrz, R.D., Hinz, P.M., Hoffmann, W.F., Hora, J.L., Mamajek, E.E., & Meyer, M.R. 2003a, AJ, 125, 1458-1466. "Mass and Kinetic Energy of the Homunculus Nebula Around Eta Carinae."
124. Smith, N., Davidson, K., Gull, T.R., Ishibashi, K., & Hillier, D.J. 2003b, ApJ, 586, 432-450. "Latitude-Dependent Effects in the Stellar Wind of Eta Carinae."
125. Smith, N., et al. 2004a, ApJ, 605, 405-424. "Kinematics and Ultraviolet to Infrared Morphology of the Inner Homunculus of Eta Carinae."
126. Smith, N., Morse, J.A., Collins, N.R., & Gull, T.R. 2004b, ApJ, 610, L105-L108. "The Purple Haze of Eta Carinae: Binary Induced Variability?"
127. Smith, N., et al. 2007, ApJ, 666, 1116-1128. "SN 2006gy: Discovery of the Most Luminous Supernova Ever Recorded, Powered by the Death of an Extremely Massive Star Like Eta Carinae."
128. Soker, N. 2001, MNRAS, 325, 584-588. "The Departure of Eta Carinae from Axisymmetry and the Binary Hypothesis."

129. Soker, N. 2004, *ApJ*, 612, 1060-1064. "Why a Single-Star Model Cannot Explain the Bipolar Nebula of Eta Carinae."
130. Soker, N. 2005, *ApJ*, 619, 1064-1071. "The Binarity of Eta Carinae and its Similarity to Related Astrophysical Objects."
131. Soker, N. 2007, *ApJ*, 661, 490-495. "Comparing Eta Carinae with the Red Rectangle."
132. Stahl, O. 1987, *A&A*, 182, 229-236. "Direct imagery of circumstellar shells around Ofpe/WN9 stars in the galaxy and in the LMC."
133. Sutton, E., Becklin, E.E., & Neugebauer, G. 1974, *ApJ*, 190, L69-L70. "34-micron Observations of Eta Carinae, G333.6-0.2, and the Galactic Center."
134. Teodoro, M., et al. 2008, *MNRAS*, 387, 564-576. "Near-infrared integral field spectroscopy of the Homunculus nebula around η Carinae using Gemini/CIRPASS"
135. Thackeray, A.D. 1949, *Obs.*, 69, 31-33. "Nebulosity Surrounding Eta Carinae."
136. Thackeray, A.D. 1953, *MNRAS*, 113, 237-238. "Note on the Brightening of Eta Carinae."
137. Thackeray, A.D. 1956, *Observatory*, 76, 154-155. "Polarization of Eta Carinae."
138. Thackeray, A.D. 1961, *Observatory*, 81, 99-104. "Spectra of the Polarized Halo Around Eta Carinae."
139. Verner, E., Bruhweiler, F., Nielsen, K.E., Gull, T.R., Viera kober, G., & Corcoran, M.F. 2005, *ApJ*, 629, 1034-1039. "Discovery of CH and OH in the -513 km s^{-1} Ejecta of Eta Carinae."
140. Visvanathan, N. 1967, *MNRAS*, 135, 275-286. "Polarization in Eta Carinae."
141. Voors, R.H.M., et al. 2000, *A&A*, 356, 501-516. "Infrared imaging and spectroscopy of the Luminous Blue Variables Wra 751 and AG Car."
142. Walborn, N.R. 1973, *ApJ*, 204, L17-L19. "The Complex Outer SHell of Eta Carinae."
143. Walborn, N.R., Blanco, B.M., & Thackeray, A.D. 1978, *ApJ*, 219, 498-503. "Proper Motions in the Outer Shell of Eta Carinae."
144. Walborn, N.R., & Liller, M. 1977, *ApJ*, 211, 181-183. "The Earliest Spectroscopic Observations of Eta Carinae and its Interaction with the Carina Nebula."
145. Walsh, J.R., & Ageorges, N. 2000, *A&A*, 357, 255-267. "High Resolution Near-Infrared Polarimetry of Eta Carinae and the Homunculus Nebula."
146. Warren-Smith, R.F., Scarrott, S.M., Murdin, P., & Bingham, R.G. 1979, *MNRAS*, 187, 761-768. "Optical Polarization Map of Eta Carinae and the Nature of its Outburst."
147. Weigelt, G., et al. 1995, *RevMexAA*, Ser. Conf., 2, 11-16. "HST FOC Observations of Eta Carinae."
148. Westphal, J.A., & Neugebauer, G. 1969, *ApJ*, 156, L45-L48. "Infrared Observations of Eta Carinae to 20 microns."
149. Whitelock, P.A., Feast, M.W., Koen, C., Roberts, G., & Carter, B.S. 1994, *MNRAS*, 270, 364-372. "Variability of Eta Carinae."
150. Woosley, S.F., Blinnikov, s., & Heger, A. 2007, *Nature*, 450, 390-392. "Pulsational Pair Instability as an Explanation for the Most Luminous Supernovae."
151. Zethson, T., et al. 1999, *A&A*, 344, 211-220. "Strange Velocities in the Equatorial Ejecta of Eta Carinae."